Naringenin ameliorates homocysteine induced endothelial damage via the AMPKα/Sirt1 pathway

Hui Li [a,d], Linlin Liu [a], Zhiwen Cao [a], Wen Li [a], Rui Liu [a], Youwen Chen [a], Chenxi Li [a], Yurong Song [a], Guangzhi Liu [a], Jinghong Hu [a,*], Zhenli Liu [c,*], Cheng Lu [b,*], Yuanyan Liu [a,*]

[a] School of Chinese Materia Medica, Beijing University of Chinese Medicine, Beijing 100029, China
[b] Institute of Basic Research in Clinical Medicine, China Academy of Chinese Medical Sciences, Beijing 100700, China
[c] Institution of Basic Theory, China Academy of Chinese Medical Sciences, Beijing 100700, China
[d] State Key Laboratory for Bioactive Substances and Functions of Natural Medicines, Beijing Key Laboratory of New Drug Mechanisms and Pharmacological Evaluation Study, Institute of Materia Medica, Chinese Academy of Medical Sciences & Peking Union Medical College, Beijing 100050, China

GRAPHICAL ABSTRACT
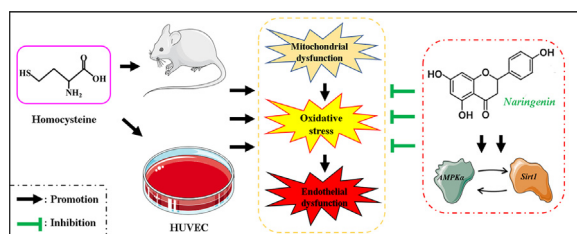
ARTICLE INFO

ABSTRACT

Introduction: Endothelial damage (ED) has been implicated in accelerating the development of atherosclerosis. The latter condition is a risk factor for developing several cardiovascular diseases (CVDs) associated with high morbidity and mortality rates worldwide.

Objectives: In our previous studies, we found naringenin (Nar), a bioactive flavanone compound, to protect against mitochondrial damage and oxidative stress. Though the pleiotropic effects of Nar have been well described, precise cytoprotective mechanisms of Nar against homocysteine (Hcy) induced ED remains elusive. Understanding these events may give an insight in to prevention and treatment of CVDs.

Methods: After ruling out the NMDA-R1 mediated pathway, RNA-Seq, a novel transcriptomic technique uncovered AMPK signaling pathway was identified as the mechanism with which Nar corrects ED. Further in vivo and in vitro tests validated the role of Nar against ED.

Results: In particular, Nar activates AMPKα/Sirt1 signaling pathway, which restores mitochondrial Ca^{2+} balance and ultimately lowered production of reactive oxygen species (ROS). Activated AMPKα/Sirt1 signaling pathway also up-regulates endothelial nitric oxide synthase (eNOS) activity, and then increasing the production of nitric oxide (NO), ultimately ameliorating ED.

Conclusion: Nar could increase the ROS elimination and decrease eNOS uncoupling, subsequently upregulate the NO bioavailability and endothelial function by activating AMPKα/Sirt1 signaling pathway.

Introduction

High plasma homocysteine (Hcy) can cause endothelial damage (ED), implicated in accelerating the development of atherosclero-

sis. On the other hand, atherosclerosis is a risk factor for several cardiovascular diseases (CVDs) such as hypertension, coronary disease, hyperlipidaemia and stroke [1]. In our previous study [2], we found total phenolic extracts of *Citrus aurantium L.* (TPE-CA) to protect against ED by balancing the production of several vascular regulatory mediators. Also, TPE-CA modulates ED by improving the remodeling and disruptions in thoracic aortas and by regulating the metabolism of arachidonic acid (AA). To further uncover more vascular protective compounds, naringenin (Nar), a major bioactive flavanone compound in TPE-CA, was systematically screened against Hcy induced ED. Intriguingly, Nar was found to have numerous pharmacological properties beneficial to human health. For instance, it is an excellent agent against oxidative stress, atherosclerosis, thrombotic and hypertension [3–4]. In a related study, Nar markedly ameliorated ischemic injury in 1-year old rats by restoring the collapsed mitochondrial membrane potential. Through these, not only was the disrupted electron transport chain restored, it also corrected ED [5].

Hcy activates N-methyl-d-aspartate receptor 1 (NMDA-R1), which promotes influx of Ca^{2+} into the endothelial cell [6]. This increases mitochondrial Ca^{2+}, will subsequently collapse membrane potential of the organelle. In the end, it disrupts electron transport chain, reducing oxygen utilization and accumulation of superoxide [7]. High levels of superoxide impairs normal metabolic process in the mitochondria [8]. On the other hand, accumulation of mitochondria-generated reactive oxygen species (ROS) release into the cytoplasm will induce oxidative stress in endothelial cell [9], Oxidative stress damage endothelial functions by down-regulating the expression of endothelial nitric oxide synthase (eNOS), and then reducing the production and bioavailability of nitric oxide (NO). Additionally, oxidative stress accelerate the accumulation of oxidized low-density lipoproteins (oxLDL) and related apoptosis and inflammation [10,11]. NO synthesized by eNOS, is an important vasodilator that additionally suppresses the expression of adhesion molecules, platelet aggregation and proliferation of vascular smooth muscle cell (VSMC) [12]. Hence, it is conceivable that improving mitochondrial function can reduce generation of superoxide and increase activity of eNOS as well as NO bioavailability. Also, inhibiting the uncoupling of eNOS can potently prevent development of ED.

Silent information regulator 1 (Sirt1), a multifunctional nicotinamide adenine dinucleotide (NAD^+) dependent protein deacetylase, is the most well-known member of SIRT family [13]. Substantial evidences show that Sirt1 plays an essential role in energy metabolic homeostasis, protection of mitochondrial functions and modulation of oxidative stress. It achieves these by activating deacetylation of its associated or downstream proteins such as AMP-activated protein kinase (AMPK), eNOS and peroxisomal proliferators-activated receptor γ-coactivator-1α (PGC-1α) [14–15]. Moreover, recent studies show that Sirt1 mediates several beneficial biological functions in human organism, including prolongs the lifespan and prevents development of CVDs [16]. On the other hand, AMPK is a member of the SNF1/AMPK protein kinase family that regulates cellular metabolic process. AMPK induces ATP production in response low ATP/AMP ratio [17]. Intriguingly, activation of AMPKα, an AMPK subunit, inhibits production of mitochondrial-induced ROS by regulating the mitochondrial electron transport chain and increasing secretion of superoxide dismutase (SOD) [18]. In addition, activated AMPKα phosphorylates eNOS at position ser1177, thus up-regulating expression of the enzyme. Activation of eNOS up-regulates NO production, which improves endothelial function [19]. Therefore, we speculated that activation of AMPKα/Sirt1 signaling pathway could modulate ED induced by mitochondrial dysfunction, oxidative stress and eNOS inactivation.

RNA sequencing (RNA-seq) is an emerging transcriptomic technique for analyzing expression of proteins both in prokaryotes and eukaryotes [20]. It is gradually known as the preferred methods in gene expression study field ascribed to the incremental progress in techniques and platforms of bioinformatics analysis [21]. Through RNA-seq, novel transcriptional factors in the transcriptional networks have been uncovered [22]. In addition, gene enrichment analysis further reveals the molecular function of differentially expressed genes (DEGs) and their associated biological pathways [22]. Accordingly, RNA-seq has been widely used in identifying potential molecular targets and pathways of natural compounds [23–25].

The aim of this study was to evaluate the potential protective property of Nar against Hcy induced ED and the probable underlying cytoprotective mechanisms both in vivo and in vitro. The first experiment demonstrated that Nar exerted its anti-oxidative stress effect without modulating NMDA-R1 mediated L-type voltage-gated calcium channel in HUVECs. Consequently, we used high-throughput RNA-Seq profiling to unearth Nar mediated mechanism against Hcy induced ED. The RNA sequence analysis revealed AMPKα/Sirt1 signaling pathway was the main pathway with which Nar exerts its cytoprotective function. As such, we performed both in vivo and in vitro experiments to validate this preliminary discovery.

Materials and method

Reagents and antibodies

Naringenin (B21596, for in vitro experiments, purity > 98%, ASB-00014206–001, for in vivo experiments, purity > 98%) and homocysteine (S20422, purity > 90%) were purchased from Shanghai Source Leaf Biological Technology Co., Ltd. Endothelial cell medium (SC-1001) was sourced from ScienCell, Fluo-3 AM (F8841). HEPES buffer saline and Hank's balanced salt solution (H1025) were purchased from Beijing Solarbio Science & Technology Co., Ltd. MitoSOX™ red mitochondrial superoxide indicator (M36008), TRIzol™ reagent (15596026), trypsin (15050065), Lipofectamine™ RNAiMAX Transfection Reagent (13778100), Opti-MEM™ I Reduced Serum Medium (31985070), siRNA included PRKAA1 (s101), SIRT1 (s223592) and Silencer™ Select Negative Control No. 1 siRNA (4390843) were purchased from Thermo Fisher Scientific (MA, USA). Antibodies; anti-AMPKα (D5A2), anti-Sirt1 (C14H4), anti-NMDA-R1 (D65B7) and anti-GAPDH (D4C6R) were sourced from Cell Signaling Technology, whereas anti-eNOS (ab76198) was purchased from Abcam.

Cell culture

Human umbilical vein endothelial cells (HUVECs) were purchased from BeNa Culture Collection. The cells were cultured in endothelial cell medium supplemented with 10% fetal bovine serum, penicillin (100 U/mL), streptomycin (100 U/mL) and endothelial cell growth factors and incubated at 37 °C under 95% humidity and 5% CO_2 and O_2. All cells in the experiment were used after 5–7 passages upon reaching 80–90% confluence. HUVECs were then treated with either Hcy (100 μM) or Nar (200 μM) for 24 h. All experiments were repeated three times.

Cell viability assay

First, the HUVECs were seeded in a 96-well plate (1×10^4 cell/well) and cultured for 24 h, before treatment with different concentrations of Nar (12.5, 25, 50, 100, 200, 400 μM) for another 24 h. Their viability was assessed based on the counting Kit-8

(CCK-8, DOJINDO laboratories). Briefly, 100 μl serum free cell medium supplemented with 10% CCK-8 solution was added to each well and incubated at 37 °C for 3 h. The absorbance in each well was then measured at 450 nm using a microplate reader. Cell viability calculated as follows:

$$Cell\ viability(\%) = \frac{OD_{sample} - OD_{blank}}{OD_{control} - OD_{blank}} \times 100\%$$

Establishment of ED model

To induce ED, the HUVECs were cultured for 24 h in endothelial cell medium supplemented with varied concentrations of Hcy (25, 50, 100, 200 μM). In the end, the optimal Hcy concentration based on the degree of induced oxidative stress, was selected for subsequent experiments.

Measurement of cytoplasmic and mitochondrial ROS

Production of cytoplasmic ROS in the Hcy or Nar-treated HUVECs were measured based on a reactive oxygen species assay kit (S0033, Beyotime Biotechnology). Briefly, treated HUVECs (10^5 cells/mL) were loaded with DCFH-DA (10 μM) and incubated for 20 min at 37 °C in the dark. The cells were then rinsed thrice with serum free medium. Production of mitochondrial ROS was measured by using MitoSOX™ red mitochondrial superoxide indicator (M36008, Thermo Fisher Scientific). Briefly, treated HUVECs (10^5 cells/mL) were loaded with MitoSOX™ reagent working solution (5 μM) and incubated for 10 min at 37 °C in the dark. The cells were then rinsed thrice with warm phosphate buffer saline (PBS). Photography was performed using confocal laser scanning microscope (CLSM) system and analyzed using Image-Pro software.

Measuring intracellular Ca²⁺ content

Intracellular Ca^{2+} content was measured based on the Fluo-3 AM kit (F8841, Beijing Solarbio Science & Technology Co., Ltd). Here, treated HUVECs (10^5 cells/mL) were first loaded with 5 μM of Fluo-3 AM working solution and incubated at 37 °C in dark for 30 min. The cells were gently rinsed thrice using HEPES buffer saline before another 20 min' incubation to ensure intracellular transformation of Fluo-3 AM into Fluo-3. The cells were photographed and analysed using CLSM system and the Image-Pro software, respectively.

Measurement of NO production

Production of NO in the treated HUVECs was determined using CLSM system after loading the cells with DAF-FM DA (S0019, Beyotime Biotechnology). The treated HUVECs (10^5 cells/mL) were seeded in glass bottomed dish and incubated with 5 μM of DAF-FM DA work solution. Incubation was performed at 37 °C for 20 min in the dark. The cells were then rinsed thrice using PBS, and thereafter cytoplasmic NO concentration was determined using CLSM system and Image-Pro software.

Assessment of mitochondrial membrane potential

Briefly, HUVECs were seeded in 6 well plate (10^5 cells/mL) and incubated in the dark for 20 min at 37 °C with 1 mL of JC-1 staining solution (C2006, Beyotime Biotechnology). The cells were then washed thrice using JC-1 staining buffer ($1\times$) and visualized using the CLSM system.

Determination of cytochrome c release

Cells were first centrifuged for 10 min at 1000 rpm. The supernatant was further centrifuged at 13,000 rpm for 15 min at 4 °C. The resultant supernatants were used as the cytosolic fraction. The residual precipitate containing the mitochondria was permeabilized for 15 min using 0.5% Triton X-100 in PBS. The precipitate was further centrifuged for 15 min at 13,000 rpm, and the supernatant collected used as the mitochondrial fraction. The amount of cytochrome *c* levels in cytosolic and mitochondrial fractions was measured based on the human cytochrome *c* Quantikine ELISA kit (R&D Systems, Minneapolis, MN, USA). The absorbance of the cytochrome absorbance at 450 nm and 540 nm was finally determined using a microplate reader.

Transcriptome sequencing-based analysis

Total RNA of HUVECs was extracted using TRIzol reagent. The quality of the RNA, including degradation and contamination, was assessed using 1% agarose gels. Additionally, RNA Nano 6000 assay kit and Qubit RNA assay kit were applied to detect the RNA integrity and concentration, respectively. Further details on the RNA quantification and quality check are illustrated in supplementary materials.

Quantitative RT-PCR analysis

Total RNA in HUVECs was extracted using TRIzol reagent, M−MLV reverse transcriptase was then used to synthesize the cDNA. After that, cDNA was subjected to PCR-based amplification. Real-time PCR was performed using SYBR Green PCR Master Mix (Applied Biosystems, Foster City, CA) and ABI 7500 Fast Real-Time PCR System (Applied Biosystems). All the procedures were strictly according to the manufacturer's instructions. Primer sequences of three key DEGs (AMPKα, Sirt 1 and eNOS) were designed through PrimerBank and checked by Oligonucleotide Properties Calculator, the primer sequences are as follows: AMPKα: TTTGCGTGTACGAAGGAAGAAT (Forward Primer) and CTCTGTGGAGTAGCAGTCCCT (Reverse Primer), Sirt1: AAGTTGACTGTGAAGCTGTACG (Forward Primer) and TGCTACTGGTCTTACTTTGAGGG (Reverse Primer), eNOS: TGATGGCGAAGCGAGTGAAG (Forward Primer) and ACTCATCCATACACAGGACCC (Reverse Primer), GAPDH: GACAGTCAGCCGCATCTTCT (Forward primer) and GCGCCCAATACGACCAAATC (Reverse primer). All the primers were synthesized by Sangon Biotech (Shanghai). mRNA expression data were normalized to GAPDH gene expression.

RNAi-mediated silencing of AMPKα and Sirt 1

HUVECs (10^5 cells/mL) were seeded in 6-well plates and transfected with PRKAA1 siRNA (5 nM), SIRT1 siRNA (5 nM) or siRNA (5 nM scrambled (negative control)), using the Lipofectamine™ RNAiMAX Transfection reagent, following the manufacturer's instructions. After 48 h, the expression of AMPKα and Sirt1 was determined using western blot.

Animals and experimental protocol

Male Sprague Dawley (SD) rats (n = 30; 8 weeks; 180–220 g) used in this research were purchased from Vital River Laboratory Animal Technology Co., Ltd (Beijing, rodent license No. SCXK (jing) 2016−0011). The rats were reared under highly controlled environment of temperature (22–25 °C) and light (12 h, from 6:00 am to 6:00 pm). They were fed on enough food and water. After one week of adaptation, the rats were divided randomly into three groups:

normal group, high-methionine diet group (H-Met) and Nar group. During the experimental period of eight weeks, rats in the normal group were fed on standard laboratory food and water. According to our previous publication [2], rats in H-Met and Nar group were fed on methionine (3% methionine (w/w)) enriched diet for 4 weeks to induce ED. After inducing ED, rats in Nar group and H-Met group were administered with Nar (100 mg/kg/d) and saline for 4 weeks, respectively.

Ethics statement

All experimental protocols involving animals in current study were conducted according to the ethical policies and procedures approved by the Research Ethics Committee of Institute of Basic Theory of Chinese Medicine, China Academy of Chinese Medical Sciences (Approval NO. SYXK 11–00-0039).

Sample collection

After 8-week experimental period, blood samples were collected from abdominal aorta in tube containing anticoagulants, following intraperitoneal anesthetization with 1% pentobarbital sodium. To extract plasma, blood sample were centrifuged for 15 min at 10,000 rpm under 4 °C. The Plasma was stored immediately at −80 °C. In addition, thoracic aortas of the rats were removed and cut into two sections: one part was fixed in 10% formalin for later Masson's trichrome staining whereas the other part was stored at −80 °C for western blot analysis.

Measurement of Hcy content in rat plasma

A commercially available enzyme-linked immunosorbent assay kit (H245, Nanjing Jiancheng Bioengineering Institute) was applied to measure the total plasma Hcy so as to assess the vascular endothelial damage model. All procedures were performed in accordance with the manufacturer's specifications.

Determination of antioxidant enzyme, NO production and degree of lipid peroxidation

The concentration of SOD, NO and malondialdehyde (MDA) in the plasma were measured based on Cu/Zn-SOD and Mn-SOD assay kit (S0103, Beyotime Biotechnology), total nitric oxide assay kit (S0023, Beyotime Biotechnology) and lipid peroxidation MDA assay kits (S0131, Beyotime Biotechnology), respectively, following the manufacturer's instructions.

Histopathological evaluation

Thoracic aortas samples across the three groups were fixed in 10% neutral buffered formalin and embedding in paraffin and sliced into 5 μm thick section after blocking. Histological observation and photography were performed using a light microscope (Olympus, Japan) after Masson's Trichrome staining.

Western blot analysis

Western blotting was performed as previously described [2]. Briefly, total proteins from HUVECs or thoracic aortic endothelial tissue were extracted using RIPA buffer supplemented with protease and phosphatase inhibitors cocktail (P1045, Beyotime Biotechnology). Protein concentration was determined based on the enhanced BCA protein assay kit (P0010, Beyotime Biotechnology), and stored at −80 °C for further analysis.

To evaluate protein expression level, proteins in 50 μg of the sample were separated using electrophoresis in 10% sodium dode-cyl sulfate–polyacrylamide gel electrophoresis (SDS-PAGE). The proteins were electro-transferred to polyvinylidene difluoride (PVDF) membranes and blocked for 1 h at room temperature using 5% non-fat milk. The membranes were incubated overnight at 4 °C with specific primary antibodies: anti GAPDH (1:1000 dilution), NMDA-R1 (1:1000 dilution), Sirt1 (1:1000 dilution), AMPKα (1:1000 dilution) and eNOS (1:1000 dilution). The membranes were then incubated for 1 h at room temperature with horseradish peroxidase-conjugated secondary antibodies (1:5000). Protein bands were visualized after incubating the membranes with an ECL reagent (E1050, Lablead). The intensity of the bands was measured using Image J software.

Statistical analysis

All abovementioned experiments were repeated three times for reproducibility. Data was analysed using GraphPad Prism software (version 7.00, La Jolla California USA). Difference between groups arising from single treatment were analysed using One-way analysis of variance (ANOVA). Continuous data were expressed as means ± standard deviation (SD). Since all the data in this work were normally distributed, therefore Tukey's multiple comparison tests were utilized in present study. Statistical significance was set at P-value < 0.05 or < 0.01 or < 0.001. (*p < 0.05, **p < 0.01, ***p < 0.001).

Results

Treatment dose of Nar and Hcy

CCK-8 assay (Fig. 1A) revealed that the viability of HUVEC was only affected by higher Nar dose (>400 μM). Therefore, we used 200 μM of Nar in subsequent experiments. In addition, measurement of Hcy induced ROS (Fig. 1B) revealed that ED was only induced when Hcy treatment reached at least 100 μM. Therefore, we used 100 μM of Hcy in our modelling.

Inhibition of Nar on cytoplasmic and mitochondrial ROS

As shown in Fig. 1C, Hcy treatment significantly increased production of cytoplasmic and mitochondrial ROS. However, treatment of HUVECs with Nar for 24 h, markedly decreased both cytoplasmic and mitochondrial ROS levels. This implies that Nar protects against Hcy induced ED by modulating oxidative stress.

Effects of Nar on intracellular Ca^{2+} level and NMDA-R1 expression

Intracellular Ca^{2+} level and NMDA-R1 expression were measured to explore the potential mechanism involved in antioxidative stress property of Nar. As shown in Fig. 1D and E, it was found that Hcy treatment of HUVECs significantly increased both Ca^{2+} levels and NMDA-R1 expression. However, compared with Hcy group, Nar treatment increased Ca^{2+} content by insignificant margin, and NMDA-R1 expression only reduced by 4.93%. Therefore, Nar does not exert its cytoprotective effects against Hcy induced cellular damages by regulating the L-type voltage-gated calcium channe. As such, it was imperative to explore other potential oxidative stress protective mechanism of Nar.

RNA-seq based analysis

To deeply reveal the potential molecular targets and related pathways of Nar, RNA-seq transcriptome analysis was performed to uncover potential molecular targets and related pathways by Nar (Fig. 2). Intriguingly, we found 3353 DEGs in HUVECs after
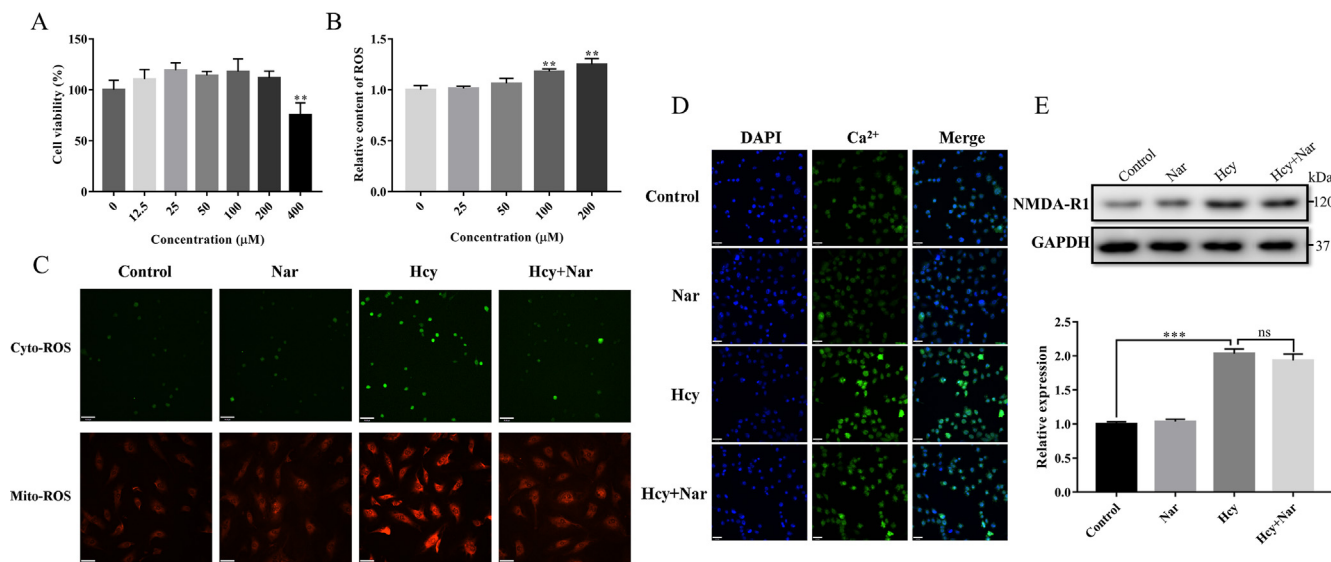
Fig. 1. Initial exploration of the potential protection and probable pathway of Nar. (A) Effects of different concentration of Nar on cell viability. (B) Effects of different concentration of Hcy on oxidative stress. (C) Effects of Nar on cytoplasmic and mitochondrial ROS. (D) Ca²⁺ level in different groups. (E) The expression level of NMDA-R1 in different groups. (Scale bar, C: 70 μm; D: 33 μm).
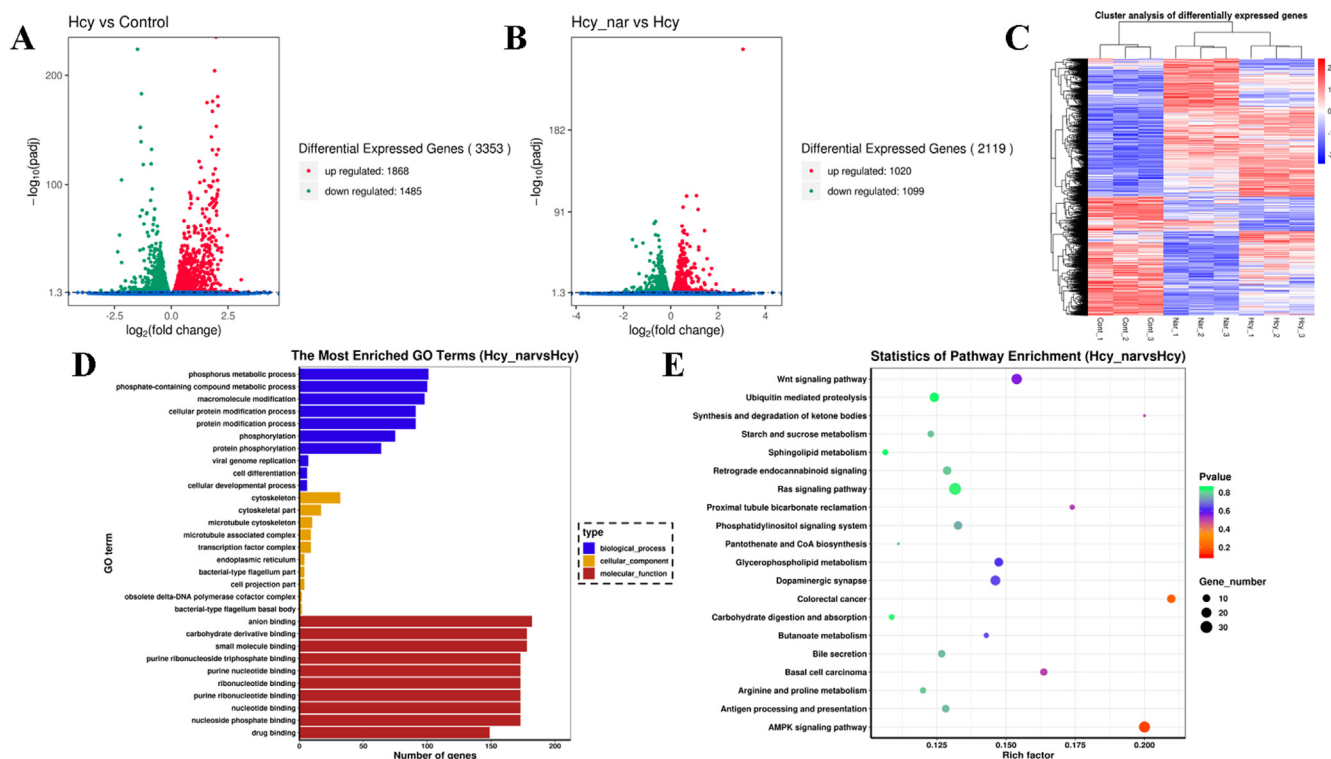

Fig. 2. RNA-seq analyses. (A) The DEGs between control and Hcy group. (B) The DEGs between Hcy and Nar group. (C) Cluster analysis of DEGs. (D) GO enrichment analysis of DEGs. (E) KEGG analysis of DEGs.

24 h treatment by Hcy, where 1868 and 1485 genes were up- and downregulated, respectively (Fig. 2A). In addition, there were 2119 DEGs between Nar group and Hcy group, in which 1020 and 1099 of them were up- and downregulated, respectively (Fig. 2B). Furthermore, cluster analysis demonstrated uniformity in DEGs in each group (Fig. 2C).

Gene Ontology (GO) analysis simultaneously performed to analyse biological processes, molecular functions and cellular components of DEGs revealed that the DEGs were mainly associated

with phosphorus and phosphate compound-containing metabolic processes (Fig. 2D). Besides, the molecular functions of the DEGs were mainly related to banding activity, such as anion and small molecules binding. Furthermore, the DEGs primarily mediated functions in the cytoskeleton and cytoskeletal regions. Finally, Kyoto Encyclopedia of Genes and Genomes ((KEGG), http://www.kegg.jp) analysis uncovered 20 pathways, including AMPK, wnt and colorectal cancer related pathways (Fig. 2E) strongly associated with DEGs. Enrichment analysis found AMPK signalling path-

way to be the most important of them in mediating the cytoprotective mechanism of Nar.

Validation of RNA-seq by quantitative RT-PCR analysis

To validate the results of RNA-seq, the mRNA level of AMPKα, Sirt1 and eNOS were detected using quantitative RT-PCR. As shown in Fig. 3 (A–C), compared with controls, Hcy treatment dramatically reduced the mRNA level of AMPKα and Sirt1, but Nar treatment recovered normal mRNA level of AMPKα and Sirt1. However, the mRNA levels of eNOS were notably reduced in both Hcy group and Nar group. These findings indicated that current methods of RNA-seq were reliable.

Nar activates AMPKα/Sirt1 signalling pathway in vitro

Based on RNA-seq analysis, we performed further analyses on AMPK signalling pathway. In particular, we measured the AMPKα, a critical protein in AMPK signalling pathway. Sirt1 and eNOS, as independent proteins that interact with AMPKα downstream of AMPK signalling pathway, were also measured. As shown in Fig. 3 (D–F), compared with controls, Hcy treatment significantly

hampered expression of Sirt1 (46%), AMPKα (35.7%) and eNOS (25%). However, Nar treatment restored normal expression of the three proteins. These findings imply that Nar activates AMPKα/Sirt1/eNOS signalling pathway in vitro.

Knockdown of AMPKα or Sirt1 abrogate the protective effects of Nar against Hcy induced ED

To strengthen the view that Nar inhibits Hcy induced oxidative stress via the AMPKα/Sirt1 pathway, AMPKα and Sirt1 knockdown in HUVECs was performed using specific siRNAs: siPRKAA1 and siSirt1, respectively. Control group was transfected with scrambled siRNA (siControl). Western blotting performed after 48 h to assess the knockdown efficacy of specific siRNAs, as shown in Fig. 4 (A–B), the present specific siRNA could notably inhibit AMPKα and Sirt1 expression in experimental groups. Meanwhile, expression of mitochondrial ROS and eNOS as well as NO, a product of the eNOS, were carefully measured. Results found that the protective effects of Nar against Hcy induced eNOS inactivation and ROS production were abolished in the siPRKAA1 and siSirt1 transfected cells (Fig. 4C–G and I). Additionally, Fig. 4H and J showed that expression of Sirt1 would be down-regulated in siPRKKA1 treatment
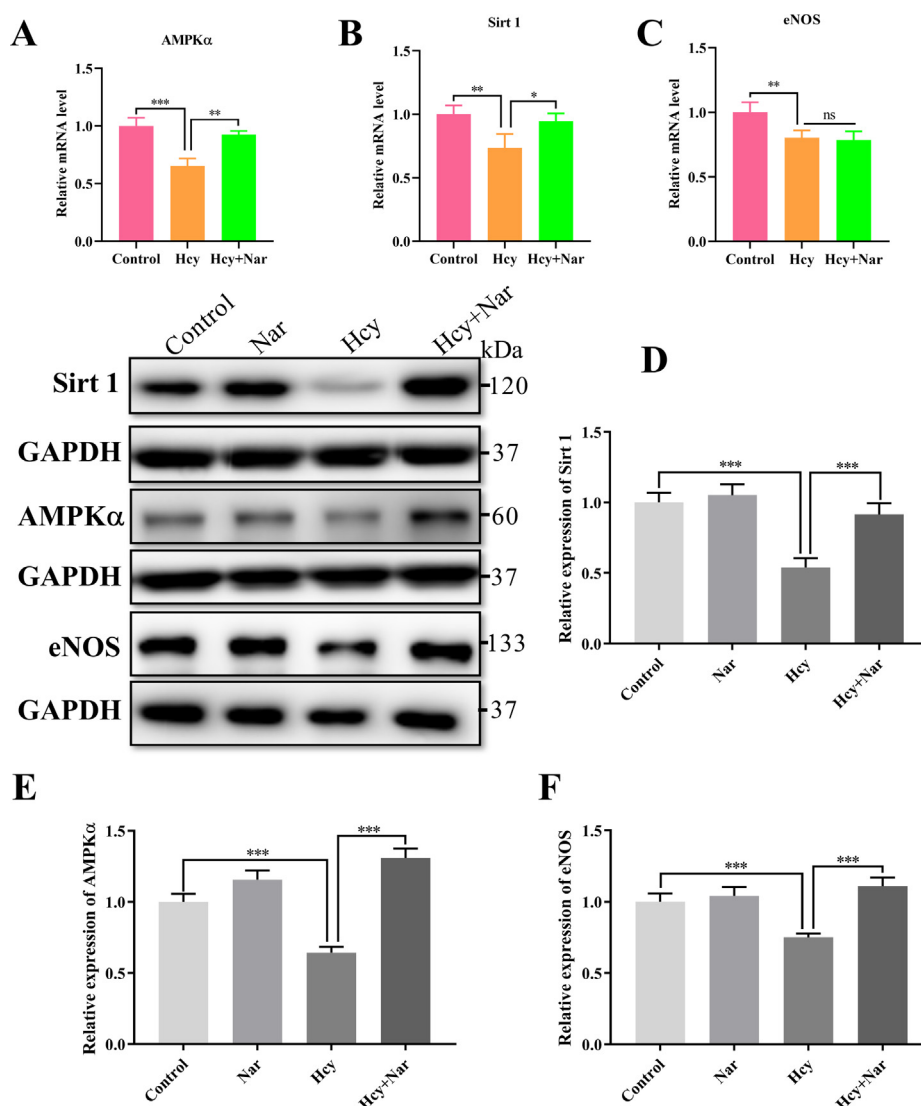

Fig. 3. Effects of Nar on AMPKα/Sirt1 signalling pathway in HUVECs. (A-C) RT-PCR results of AMPKα, Sirt 1 and eNOS. (D) The relative expression of Sirt1 in different groups. (E) The relative expression of AMPKα in different groups. (F) The relative expression of eNOS in different groups.
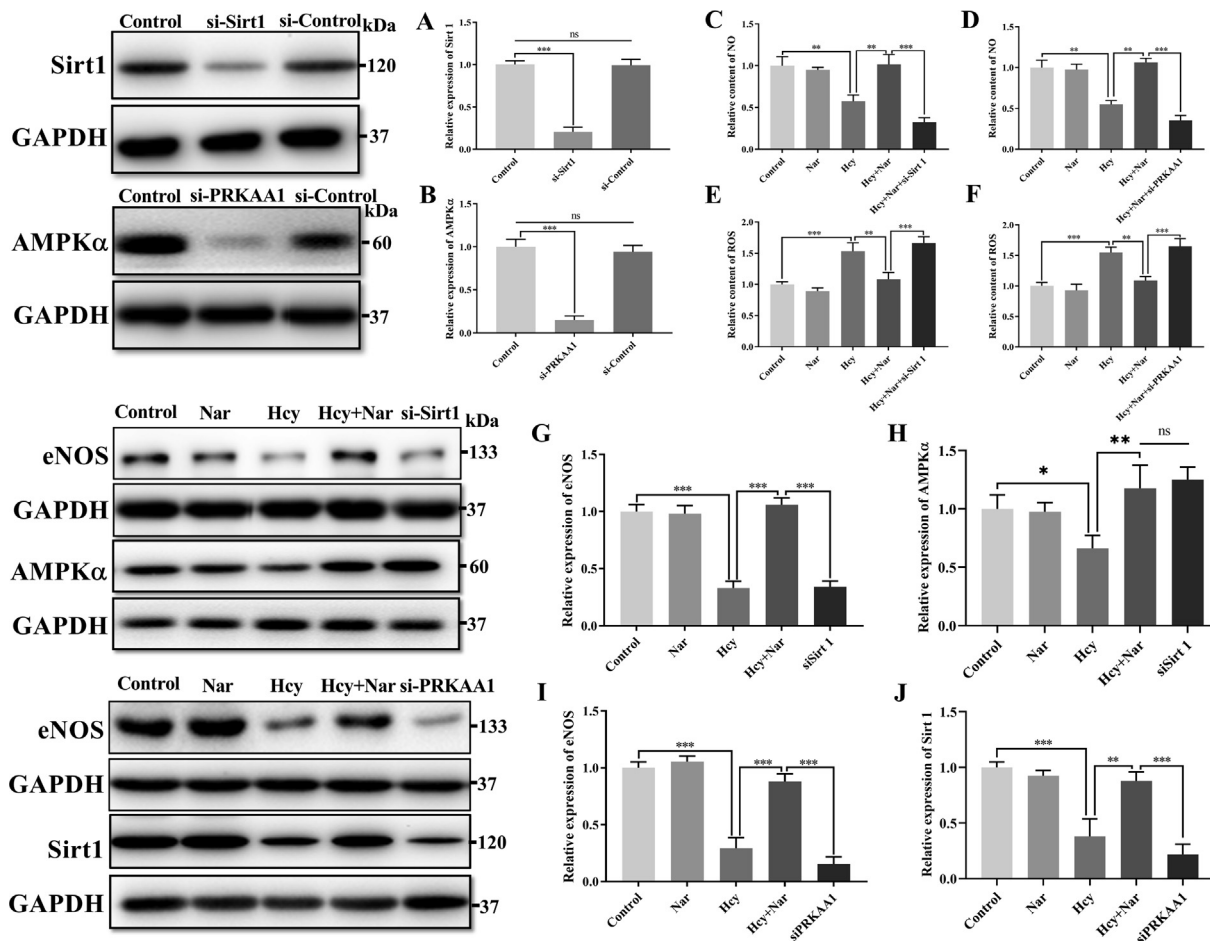
Fig. 4. Effects of siRNA transfection on AMPKα/Sirt1 signalling pathway, ROS generation and NO production. (A-B) Knockdown efficacy of AMPKα and Sirt1. (C-D) Production of NO in different group. (E-F) Relative amount of ROS in different group. (G) Relative expression of eNOS in different group. (H) Relative expression of AMPKα in different group. (I) Relative expression of eNOS in different group. (J) Relative expression of Sirt 1 in different group.

group, but expression of AMPKα was displayed insignificant alteration in siSirt1 treatment group. This implied that Sirt1 was the downstream effector protein of AMPK signalling pathway, modulated by AMPKα. Together, these findings further strengthen the view that Nar protects against Hcy induced eNOS inactivation and ROS generation via the AMPKα/Sirt1 signalling pathway.

Effects of Nar on mitochondrial dysfunction

Mitochondrial membrane electron potential is an important characteristic indicator of aggravated mitochondrial dysfunction. To explore the potential mechanism underlying Nar anti-mitochondrial dysfunction, we evaluated the changes in mitochondrial membrane potential after Nar treatment. Current data showed that Hcy treatment significantly decreased the mitochondrial membrane potential. However, Nar treatment restored normalcy. Even so, the effects of Nar on mitochondrial membrane potential significantly decreased both in siPRKAA1 and siSirt1 transfected cells (Fig. 5B). On the other hand, the expression of cytochrome *c* level, a key indicator of mitochondrial function (Fig. 5A), significantly decreased in the mitochondria but increased in the cytoplasm of Hcy-treated HUVECs. However, after 24 h Nar treatment, the level of cytoplasmic cytochrome *c* decreased, whereas that in the mitochondria increased in Hcy-treated HUVECs. These findings demonstrate that Nar could effectively

ameliorate Hcy-impaired mitochondrial function through a mitochondria dependent pathway.

Model evaluation

Hyperhomocysteinemia (HHcy) is clinically defined as plasma Hcy higher than 15 μmol/L. Substantial evidences indicate that HHcy-induced vascular endothelial damage is ascribed to an increased Hcy concentration. Therefore, the plasma Hcy concentration, as a pivotal index for model evaluating, was measured by using a commercially available Elisa kit. As shown in Fig. 5C. After fed with H-Met for 4 weeks, the levels of Hcy in rat plasma was significantly increased in H-Met group and Nar group that higher than 15 μmol/L. It indicated that the vascular endothelial damage model has been induced successfully in current experiments.

Effects of Nar on antioxidant enzyme, NO and lipid peroxidation

Because Nar had a positive in vitro effect on Hcy induced ED, animal experiments were designed to explore its effect on ED, in vivo. Compared to the normal group, the amount of SOD and NO significantly decreased in H-Met group. However, rats treated with Nar displayed higher expression of SOD and NO (Fig. 5D and E). Additionally, H-met group significantly up-regulated MDA expression, but Nar treatment corrected abnormal MDA expression
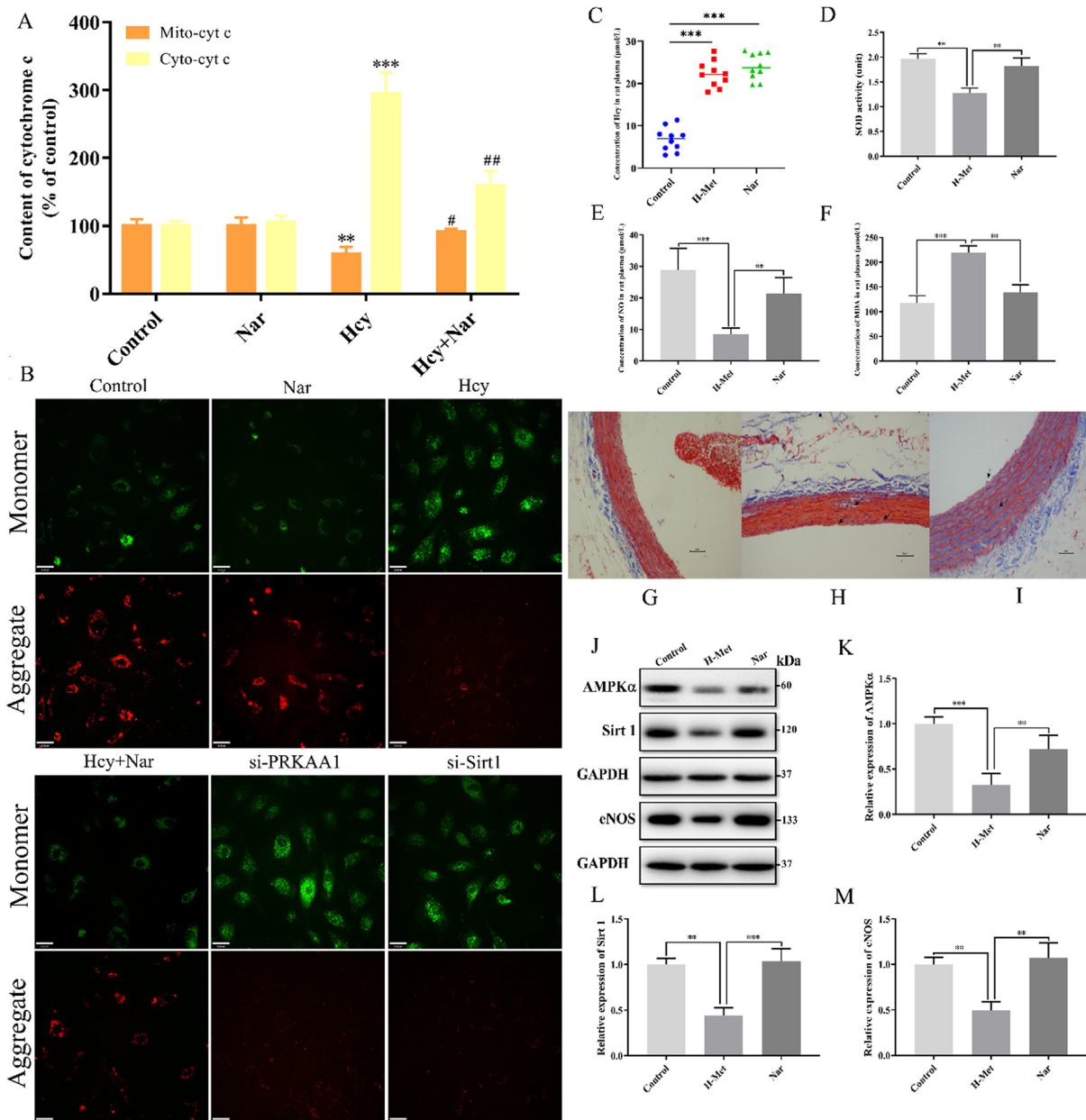
Fig. 5. Effects of Nar on mitochondrial dysfunction, histomorphology and in vivo AMPKα/Sirt1 signaling pathway. (A) Concentration of cytochrome *c* level in mitochondria or cytoplasm in different groups. (B) Mitochondrial membrane potential in different groups. (Scale bar: 33 μm). (C) Concentration of Hcy in rat plasma after H-Met fed for 4 weeks. (D) The expression level of SOD in different groups. (E) The concentration of NO in rat's plasma. (F) The concentration of MDA in rat's plasma. (G) Histopathology of thoracic aortas in control group. (H) Histopathology of thoracic aortas in H-Met group. (I) Histopathology of thoracic aortas in Nar group. Distinct histopathological characteristic in each group are indicated by arrowhead. (Scale bar = 10 μm, Magnification: 200×). (J) Western blotting analysis of AMPKα, Sirt 1 and eNOS in different groups. (K) The relative expression of AMPKα in different group. (L) The relative expression of Sirt 1 in different group. (M) The relative expression of eNOS in different group.

(Fig. 5F). These findings validated the in vivo anti-oxidative stress property of Nar against ED.

Histopathological evaluation

Masson's trichrome staining (Fig. 5G–I) revealed that the vascular walls of thoracic aorta of rats in the normal group exhibited the custom histology, composed of adventitia, middle and inner layers (Fig. 5G). However, the normal histoarchitecture was disrupted in H-Met group, with degraded myofiber and dissolved collagen (Fig. 5H). Nar group displayed significantly visible recoveries for myofiber disruption, collagen ratio and vascular wall architecture (Fig. 5I). These findings imply that Nar treatment can effectively

ameliorate and restore Hcy induced damaged vascular walls of thoracic aorta.

Effects of Nar on AMPKα/Sirt1 signaling pathway

Because Nar up-regulated AMPKα/Sirt1 signaling pathway and the expression of key proteins including AMPKα, Sirt1 and eNOS in HUVECs, we evaluated its effect on the same parameters in vivo. Here, expression of AMPKα, Sirt1 and eNOS were inhibited in H-Met group, consistent with findings of cell experiments. However, Nar treatment restored normal expression of the three proteins (Fig. 5J–K). These results confirmed that Nar can activate the AMPKα/Sirt1/eNOS signaling pathway in vivo.

Discussion

Currently, approximate one third of western population suffer from various CVDs, mainly induced by vascular endothelial dysfunction. ED is a structural and functional impairment of vascular endothelial layer, characterized by decrease in eNOS expression but increase in production of ROS which together, impair vasodilation of blood vessels [26,27]. Endothelial damage leads to atherosclerosis, a progressive vascular pathological disease that ultimately leads to various CVDs [10]. High ROS impairs electron transport chain in the mitochondria, as well as increases production of ROS in a malignant feedback manner. Excess ROS released in the cytoplasm from the mitochondria combine with cytoplasmic NO to form harmful peroxynitrite that reduces NO bioavailability [28]. Intriguingly, our previous study found that TPE-CA, a kind of mixture containing more than 20% Nar and its derivatives, exerted various beneficial effects against ED. Therefore, a deeper understanding of mechanism underlying the amelioration of Nar on Hcy induced ED may give an insight on prevention and treatment of CVDs.

Accumulating evidences suggested that Hcy up-regulate expression of NMDA-R1. It can also activate L-type voltage-gated calcium channel which increases concentration of Ca^{2+} both in the cytoplasm and mitochondria. Because high levels of Ca^{2+} polarize the cell, it impairs mitochondrial functions, thus increasing production of ROS. This study demonstrated that Hcy treatment significantly up-regulated NMDA-R1 activity and cytoplasmic Ca^{2+}, consistent with previous studies [6]. In addition, both cytoplasmic and mitochondrial ROS levels markedly increased in response of Hcy. Intriguingly, after 24 h Nar treatment, the level of cytoplasmic and mitochondrial ROS decreased significantly. However, the decrease in Ca^{2+} concentration and NMDA-R1 expression were insignificant. Here, although Nar effectively reduce production of ROS, the precise mechanism underlying this property remained elusive.

Meanwhile, RNA-Seq is new genomic analysis technique useful in identifying potential molecular targets and associated pathways for human disease, microbial pathogens and drugs discovery [22]. RNA-Seq was employed in this study to unravel potential pathways with which Nar correct ED. Our analysis revealed that AMPK signalling pathway was suddenly activated by Nar treatment. KEGG map further revealed that AMPKα and Sirt 1, key proteins in the AMPK signalling pathway, were also up-regulated. AMPK signalling pathway mediates several beneficial functions. Among them, AMPK regulates ATP production and maintains redox potential that ensures optimal mitochondrial functioning [29]. In particular, phosphorylation of downstream eNOS protein at position ser1177 site by up-regulated AMPKα increases eNOS expression and NO production, which ameliorates ED [19]. Consequently, we assessed the expression of AMPKα, Sirt 1 and eNOS under varied conditions. We found Hcy treatment significantly decreased expression of AMPKα, Sirt 1 and eNOS in HUVECs. However, Nar treatment greatly reversed the inhibiting effect of Hcy, and up-regulated proteins mentioned above. Meanwhile, PCR data showed that Nar treatment could only transcriptionally regulate the expression of AMPKα and Sirt1, but not eNOS. So, we speculated that activation of eNOS in this study might due to the phosphorylation of ser1177 site of eNOS by AMPKα, rather than being directly activated by Nar. These findings in part underlined the usefulness of RNA-Seq in uncovering novel molecular pathways. Overall, our findings demonstrated that Nar protect against oxidative stress by up-regulating the expression of eNOS, through the AMPKα/Sirt1 signaling pathway. Additionally, it is well known that ubiquitin proteasome system is a catalytic machinery that targets numerous cellular proteins for degradation, thus being essential to control a wide range of basic cellular processes and cell survival. According to current results, we thus inferred that Nar treatment might inhibit the ubiquitination degradation of eNOS such as PKCα ubiquitination signal pathway, which have been confirmed to regulate the expression of eNOS [30]. Therefore, although Nar treatment did not transcriptionally regulate the mRNA expression of eNOS, inhibition of the ubiquitination signal pathway by Nar treatment may increase the eNOS protein expression. However, the deeper and exact ubiquitination mechanisms should be furtherly explored and verified in future work.

To further validate the role of AMPKα/Sirt1 signaling pathway in regulating oxidative stress in HUVECs with ED, expression of AMPKα and Sirt1 were specifically knocked down through two highly specific siRNAs. Western blotting was performed after 48 h of transfection to assess the efficiency of AMPKα and Sirt1 inhibition. Intriguingly, favorable modulation of Nar on ROS levels, eNOS expression and NO bioavailability were thoroughly impaired in cells not expressing AMPKα and Sirt1. In cells, mitochondria generate ATP, sequestrates Ca^{2+} and generates and detoxifies cellular ROS [31,32]. Given the susceptibility of mitochondrial function to oxidative stress, we assessed mitochondrial membrane potential as well as the concentration of cytoplasmic and mitochondrial cytochrome *c*. Results demonstrated that Nar treatment restored the mitochondrial membrane potential and modulated excessive release of mitochondrial cytochrome *c* into the cytoplasm. Collectively, these findings demonstrate that Nar also improves mitochondrial function and suppresses oxidative stress. It achieves these by enhancing the mitochondrial membrane potential, reducing the release of mitochondrial cytochrome *c* and activating AMPKα/Sirt1 signaling pathway.

Apart from in vitro tests, animal experiments were performed to furtherly validate the protective effects and potential mechanisms of Nar against ED. First, we measured the amount of SOD, MDA and NO in rat's plasma to provide a preliminary idea of oxidative stress and endothelial function in different groups. SOD is an antioxidant enzyme that catalyzes conversion of O_2 into hydrogen peroxide (H_2O_2). MDA is a product of the lipid peroxidation, useful in assessing the degree of oxidative stress in cells [33]. In this study, Nar treatment significantly up-regulated secretion of SOD and production of NO, but markedly inhibited MDA production. Masson's trichrome staining further revealed that Nar treatment healed Hcy-damaged vascular endothelial walls by restoring myofiber disruptions, collagen ratio imbalance and structural changes. Also, Nar therapy significantly activated AMPKα/Sirt1 signaling pathway, consistent with in vivo experiments. Collectively, our findings demonstrated that Nar treatment can protect against oxidative stress, ameliorate ED and vascular wall damage through several mechanisms. In particular, Nar enhances expression of enzymatic antioxidants, reduces lipid peroxidation, restores vascular wall histoarchitecture and activates AMPKα/Sirt1 signaling pathway.

Conclusion

To our knowledge, this is the first study demonstrating the therapeutic potential and related mechanisms of Nar against Hcy induced ED using a combination of in vivo and in vitro experiments. After ruling out the NMDA-R1 mediated pathway, RNA-Seq, a novel transcriptomic technique uncovered AMPK signaling pathway was identified as the mechanism with which Nar corrects ED. In particular, Nar activates AMPKα/Sirt1 signaling pathway, which restores mitochondrial Ca^{2+} balance and ultimately lowered production of ROS. Activated AMPKα/Sirt1 signaling pathway also up-regulates proteins downstream of eNOS. This increases the production of NO, ultimately ameliorating ED (Fig. 6). Furthermore,
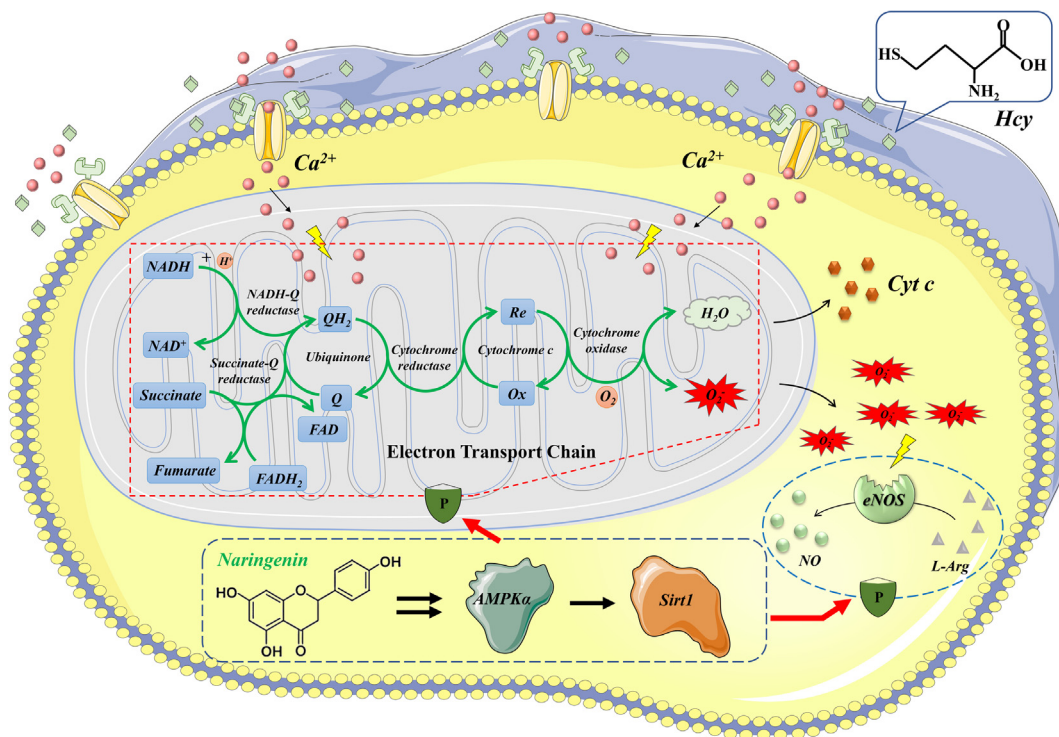
Fig. 6. The schematic diagram of therapeutic mechanism of Nar against Hcy induced endothelial dysfunction. Obviously, Nar can elevate AMPKα/Sirt1 signaling pathway consequently rescue the Ca²⁺ disrupted mitochondrial function and reduce the ROS production. Furthermore, activated AMPKα/Sirt1 signaling pathway will upregulate the activity of downstream protein of eNOS subsequently increase the production of NO, ultimately ameliorate the ED.

these conclusions were mutually verified in animal experiments, indicating that Nar could increase the ROS elimination and decrease eNOS uncoupling, subsequently upregulate the NO bioavailability and endothelial function by activating AMPKα/Sirt1 signaling pathway. In studies to follow, we shall perform structural biological studies to gain a deeper understanding on the structural mechanism of Nar activates AMPKα.

Compliance with Ethics Requirements

All Institutional and National Guidelines for the care and use of animals (fisheries) were followed.

Declaration of Competing Interest

The authors declare that they have no known competing financial interests or personal relationships that could have appeared to influence the work reported in this paper.

Acknowledgments

References

[1] Jamwal S, Sharma S. Vascular endothelium dysfunction: a conservative target in metabolic disorders. Inflam Res: Off J Eur Histamine Res Soc 2018;67(5):391–405.
[2] Li H, Liu Z, Liu L, Li W, Cao Z, Song Z, et al. Vascular protection of TPE-CA on hyperhomocysteinemia-induced vascular endothelial dysfunction through AA metabolism modulated CYPs pathway. Int J Biol Sci 2019;15(10):2037–50.
[3] Mulvihill EE, Assini JM, Sutherland BG, DiMattia AS, Khami M, Koppes JB, et al. Naringenin decreases progression of atherosclerosis by improving dyslipidemia in high-fat-fed low-density lipoprotein receptor-null mice. Arterioscler Thromb Vasc Biol 2010;30(4):742–8.
[4] Liu Y, An W, Gao A. Protective effects of naringenin in cardiorenal syndrome. J Surg Res 2016;203(2):416–23.
[5] Testai L, Da Pozzo E, Piano I, Pistelli L, Gargini C, Breschi MC, et al. The citrus flavanone naringenin produces cardioprotective effects in hearts from 1 year old rat, through activation of mitoBK channels. Front Pharmacol 2017;8:71.
[6] Ostrakhovitch EA, Tabibzadeh S. Homocysteine and age-associated disorders. Ageing Res Rev 2019;49:144–64.
[7] Vacek TP, Vacek JC, Tyagi SC. Mitochondrial mitophagic mechanisms of myocardial matrix metabolism and remodelling. Arch Physiol Biochem 2012;118(1):31–42.
[8] Sobenin IA, Chistiakov DA, Bobryshev YV, Postnov AY, Orekhov AN. Mitochondrial mutations in atherosclerosis: new solutions in research and possible clinical applications. Curr Pharm Des 2013;19(33):5942–53.
[9] Li J, Li J, Wei T, Li J. Down-regulation of MicroRNA-137 improves high glucose-induced oxidative stress injury in human umbilical vein endothelial cells by up-regulation of AMPKalpha1. Cell Physiol Biochem: Int J Exp Cell Physiol, Biochem, Pharmacol 2016;39(3):847–59.
[10] Tsai KL, Hung CH, Chan SH, Hsieh PL, Ou HC, Cheng YH, et al. Chlorogenic acid protects against oxLDL-induced oxidative damage and mitochondrial dysfunction by modulating SIRT1 in endothelial cells. Mol Nutr Food Res 2018;62(11):e1700928.
[11] Stuhlinger MC, Tsao PS, Her JH, Kimoto M, Balint RF, Cooke JP. Homocysteine impairs the nitric oxide synthase pathway: role of asymmetric dimethylarginine. Circulation 2001;104(21):2569–75.
[12] Chen JY, Ye ZX, Wang XF, Chang J, Yang MW, Zhong HH, et al. Nitric oxide bioavailability dysfunction involves in atherosclerosis. Biomed Pharmacother 2018;97:423–8.
[13] Li D, Wang X, Huang Q, Li S, Zhou Y, Li Z. Cardioprotection of CAPE-oNO2 against myocardial ischemia/reperfusion induced ROS generation via regulating the SIRT1/eNOS/NF-kappaB pathway in vivo and in vitro. Redox Biol 2018;15:62–73.
[14] Lagouge M, Argmann C, Gerhart-Hines Z, Meziane H, Lerin C, Daussin F, et al. Resveratrol improves mitochondrial function and protects against metabolic disease by activating SIRT1 and PGC-1alpha. Cell 2006;127(6):1109–22.
[15] Alcendor RR, Gao S, Zhai P, Zablocki D, Holle E, Yu X, et al. Sirt1 regulates aging and resistance to oxidative stress in the heart. Circ Res 2007;100(10):1512–21.
[16] Chan SH, Hung CH, Shih JY, Chu PM, Cheng YH, Lin HC, et al. Exercise intervention attenuates hyperhomocysteinemia-induced aortic endothelial oxidative injury by regulating SIRT1 through mitigating NADPH oxidase/LOX-1 signaling. Redox Biol 2018;14:116–25.
[17] Xu Q, Si LY. Protective effects of AMP-activated protein kinase in the cardiovascular system. J Cell Mol Med 2010;14(11):2604–13.

[18] Karnewar S, Vasamsetti SB, Gopoju R, Kanugula AK, Ganji SK, Prabhakar S, et al. Mitochondria-targeted esculetin alleviates mitochondrial dysfunction by AMPK-mediated nitric oxide and SIRT3 regulation in endothelial cells: potential implications in atherosclerosis. Sci Rep 2016;6:24108.

[19] Gao F, Chen J, Zhu H. A potential strategy for treating atherosclerosis: improving endothelial function via AMP-activated protein kinase. Sci China Life Sci 2018;61(9):1024–9.

[20] Tirosh I, Izar B, Prakadan SM, Wadsworth 2nd MH, Treacy D, Trombetta JJ, et al. Dissecting the multicellular ecosystem of metastatic melanoma by single-cell RNA-seq. Science 2016;352(6282):189–96.

[21] Hoeijmakers WA, Bártfai R Fau - Stunnenberg HG, Stunnenberg HG. Transcriptome analysis using RNA-Seq. (1940-6029 (Electronic)).

[22] Muhammad II, Kong SL, Akmar Abdullah SN, Munusamy U. RNA-seq and ChIP-seq as complementary approaches for comprehension of plant transcriptional regulatory mechanism. Int J Mol Sci. 2019;21(1).

[23] Hu R, Wang MQ, Ni SH, Wang M, Liu LY, You HY, et al. Salidroside ameliorates endothelial inflammation and oxidative stress by regulating the AMPK/NF-kappaB/NLRP3 signaling pathway in AGEs-induced HUVECs. Eur J Pharmacol 2020;867:172797.

[24] Li Y, Li N, Shi J, Ahmed T, Liu H, Guo J, et al. Involvement of glutathione depletion in selective cytotoxicity of oridonin to p53-mutant esophageal squamous carcinoma cells. Front Oncol 2019;9:1525.

[25] Zheng Z, Wu M, Zhang J, Fu W, Xu N, Lao Y, et al. The natural compound neobractatin induces cell cycle arrest by regulating E2F1 and Gadd45alpha. Front Oncol 2019;9:654.

[26] Qaradakhi T, Matsoukas MT, Hayes A, Rybalka E, Caprnda M, Rimarova K, et al. Alamandine reverses hyperhomocysteinemia-induced vascular dysfunction via PKA-dependent mechanisms. Cardiovasc Ther 2017;35(6).

[27] Azul L, Leandro A, Boroumand P, Klip A, Seica R, Sena CM. Increased inflammation, oxidative stress and a reduction in antioxidant defense enzymes in perivascular adipose tissue contribute to vascular dysfunction in type 2 diabetes. Free Radical Biol Med 2020;146:264–74.

[28] Minami T, Satoh K, Nogi M, Kudo S, Miyata S, Tanaka S, et al. Statins up-regulate SmgGDS through beta1-integrin/Akt1 pathway in endothelial cells. Cardiovasc Res 2016;109(1):151–61.

[29] Wang MJ, Peng XY, Lian ZQ, Zhu HB. The cordycepin derivative IMM-H007 improves endothelial dysfunction by suppressing vascular inflammation and promoting AMPK-dependent eNOS activation in high-fat diet-fed ApoE knockout mice. Eur J Pharmacol 2019;852:167–78.

[30] He A, Zuo D, Liang X, Guo Y, Suxin L, Xia Y. Hypoglycemia increases endothelial-dependent vasodilation through suppressing phosphorylation at Threonine 495/497 site of endothelial nitric oxide synthase. Microvasc Res. 2021;133:104075.

[31] Brand MD, Affourtit C, Esteves TC, Green K, Lambert AJ, Miwa S, et al. Mitochondrial superoxide: production, biological effects, and activation of uncoupling proteins. Free Radical Biol Med 2004;37(6):755–67.

[32] Xi Q, Cheranov SY, Jaggar JH. Mitochondria-derived reactive oxygen species dilate cerebral arteries by activating Ca2+ sparks. Circ Res 2005;97(4):354–62.

[33] He D, Liu Z, Wang M, Shu Y, Zhao S, Song Z, et al. Synergistic enhancement and hepatoprotective effect of combination of total phenolic extracts of Citrus aurantium L. and methotrexate for treatment of rheumatoid arthritis. Phytotherapy Res: PTR 2019;33(4):1122–33.